frontiers | Frontiers in Marine Science

TYPE Original Research
PUBLISHED 13 September 2024
DOI 10.3389/fmars.2024.1416421

OPEN ACCESS

EDITED BY
Khan M. G. Mostofa,
Tianjin University, China

REVIEWED BY
Ruifeng Zhang,
Shanghai Jiao Tong University, China
Anirban Akhand,
Deakin University, Australia

*CORRESPONDENCE
Jørgen Bendtsen
jorgen.bendtsen@sund.ku.dk

RECEIVED 14 May 2024
ACCEPTED 21 August 2024
PUBLISHED 13 September 2024

CITATION
Bendtsen J, Daugbjerg N and Hansen JLS (2024) Glacial rock flour increases photosynthesis and biomass of natural phytoplankton communities in subtropical surface waters: a potential means of action for marine CO_2 removal.
Front. Mar. Sci. 11:1416421.
doi: 10.3389/fmars.2024.1416421

Glacial rock flour increases photosynthesis and biomass of natural phytoplankton communities in subtropical surface waters: a potential means of action for marine CO_2 removal

Jørgen Bendtsen[1]*, Niels Daugbjerg[2] and Jørgen L. S. Hansen[3]

[1]Centre for Rock Flour Research, Globe Institute, University of Copenhagen, Copenhagen K, Denmark, [2]Marine Biological Section, Department of Biology, University of Copenhagen, Copenhagen Ø, Denmark, [3]Department of Ecoscience, Aarhus University, Roskilde, Denmark

Photosynthesis by phytoplankton reduces partial pressure of CO_2 at the surface of the ocean and is therefore a potential means of action for a marine CO_2 removal technology. Here we study how glacial rock flour may influence photosynthesis in the open ocean. Glacial rock flour is a fine-grained silicate mineral from the bedrock grinded by the Greenland Ice Sheet and enters the ocean via fjords and coastal waters. It is therefore a natural source of nutrients and trace metals to the ocean. It is easily accessible in large quantities and could be a suitable source for large-scale CO_2 removal. The impact of suspended glacial rock flour was analyzed through 14 incubation experiments with natural phytoplankton communities sampled in the subtropical Atlantic. A significant increase in photosynthesis was found in 12 experiments where variable fluorescence Fv/Fm increased 12% and the average concentration of chlorophyll *a* increased significantly in comparison with control treatments during a 6-day period. Incubations with glacial rock flour showed a significant uptake of phosphorus whereas the average concentrations of silicate and dissolved inorganic nitrogen increased. Nutrient changes could be explained by increasing phytoplankton and microbial biomass, remineralization of organic matter, and weathering (mobilization) of glacial rock flour. These short time experiments indicated that trace metals from glacial rock flour stimulated phytoplankton growth. Thus, glacial rock flour has the potential to increase photosynthesis and phytoplankton growth, and therefore may be a potential means of action for marine CO_2 removal.

KEYWORDS

marine CO2 removal, glacial rock flour, biological pump, alkalinization, phytoplankton, trace metals, iron limitation

1 Introduction

Marine carbon dioxide removal (mCDR) has a large potential for sequestering atmospheric CO_2 due to the oceanic storage capacity and its large reservoir of dissolved inorganic carbon (DIC) of ~38,000 PgC, i.e., about 40 times larger than the current atmospheric carbon pool of ~870 PgC (Canadell et al., 2021). Oceanic CO_2 uptake can be enhanced by biological primary production where DIC is synthesized to organic matter by phytoplankton in the illuminated surface layer and subsequently sinks deep into the ocean interior. Oceanic CO_2 uptake can also be enhanced by altering the chemistry of the carbonate system at the surface, e.g., increasing surface alkalinity. Both processes reduce the partial pressure of CO_2 (pCO_2) in the surface water, and thereby tend to increase the oceanic uptake of atmospheric CO_2. In addition, both methods counteract ocean acidification in the upper ocean.

Experiments have shown that phytoplankton growth in the open ocean can be stimulated by adding limiting nutrients or trace metals, e.g., iron (de Baar et al., 2005; Boyd et al., 2007), or from combinations of limiting nutrients and trace metals, e.g., phosphorus and iron (Mills et al., 2004). The feasibility of increasing biological production with the purpose of permanently sequestering atmospheric CO_2 is still debated and several aspects of altering biological carbon transport, i.e., the biological pump, require further studies (Yoon et al., 2018; NASEM, 2021). However, the large oceanic carbon storage capacity makes mCDR a promising technology for controlling atmospheric CO_2 in the coming centuries (NASEM, 2021), and may contribute to the large-scale CO_2-sequestration that is a prerequisite for keeping global warming below 1.5°C (IPCC, 2018) in accordance with the Paris-agreement (2015). Hence, research and improved methods to increase biologically mediated carbon transport from the ocean surface layer have to be developed before mCDR methods can be implemented in large-scale experiments.

Here we investigate the potential for using glacial rock flour (GRF) as a source for mCDR. GRF is a natural source of nutrients and trace metals from continental runoff to the oceans, and currently more than 8% of the global continental mass transport to the open ocean is associated with glacial rock flour transported as suspended matter into coastal waters around Greenland (Overeem et al., 2017; Andresen et al., 2024). GRF is a felsic silicate mineral abraded from the bedrock below the glaciers. It is a fine-grained material (d_{50} ~2-5 µm) that is transported via meltwater rivers, lakes or directly into the fjords via subglacial discharge at marine terminating glaciers. The small grain size implies low settling velocities and therefore a relatively large residence time near the surface, e.g., suspended plumes of GRF-material are often seen from satellites more than 100 km from its source. The large volume to surface ratio of small grain size implies a relatively fast weathering in seawater and makes it more accessible as a source for biological mobilization of nutrients. Mercury concentrations are very low in meltwater from glacial outlets from Greenland (Jørgensen et al., 2024) in accordance with the analyzed composition of GRF (Sarkar, 2021). Sarkar (2021) also found that other toxic substances in GRF from different locations around Greenland were present in very low concentrations, and comparable or below typical concentrations found in soil (e.g., concentrations in the applied GRF-material of potentially toxic elements as As and Mo were ~1.2 and 0.8 ppm, respectively, and less than the corresponding typical concentrations in soil of ~6 and 2 ppm). However, potential toxic effects from GRF on the marine biota also must be investigated before experiments are carried out in the field.

Terrestrial field-experiments have documented a positive effect from GRF on crop yield (Gunnarsen et al., 2023), and an increased CO_2 uptake due to weathering of the silicate minerals (Dietzen and Rosing, 2023). GRF could correspondingly be a source of nutrients and trace metals for stimulating biological production in the open ocean. Besides being a part of the natural cycling of nutrients between continents and the ocean it may also be an efficient way to increase ocean productivity, because marine organisms have had the time to optimize their usage of this multi-composite material, containing many different minerals and substances, on evolutionary time scales. Whether similar positive effects as seen on crop yields also is representative for its impact on phytoplankton in the marine environment is presently unknown.

This study focuses on the potential use of GRF to increase ocean productivity. This is a primary process to investigate before it is applied as a source for an mCDR technology involving the biological pump. Whether the increased productivity leads to a drawdown of atmospheric CO_2, i.e., a key component for validating the efficiency of an mCDR activity, is left for further studies. Here we study the effect from GRF by shipboard laboratory experiments carried out in the Canary Current in the subtropical Atlantic. First, we describe the incubation experiments where GRF was added to water samples with natural phytoplankton communities for determining the impact on growth, photosynthetic efficiency and nutrient budgets. Secondly, we analyze the sensitivities found in the incubation experiments and finally we discuss the potential for using GRF as a means of action for mCDR.

2 Methods

2.1 Study area

Incubation experiments with natural plankton communities in surface water (upper ~100 m) was carried out onboard the schooner, Activ, (length 42 m, draft 3 m) in the Canary Current ~100 km south of the Canary Islands (Figure 1). In total 14 experiments (Exp 1 - Exp 14, Table 1) with water samples from 13 different stations and depth levels were incubated during the period 13-29 June 2022. Water samples were incubated from open ocean areas where the depth was deeper than 3000 m.

Incubation experiments (1-2 experiments per day) were started and followed while at sea. In general, the weather conditions were good with clear sky and relatively windy conditions (> 10 m s^{-1}) due to the tunneling effect of the trade wind from the Islands. The

10.3389/fmars.2024.1416421

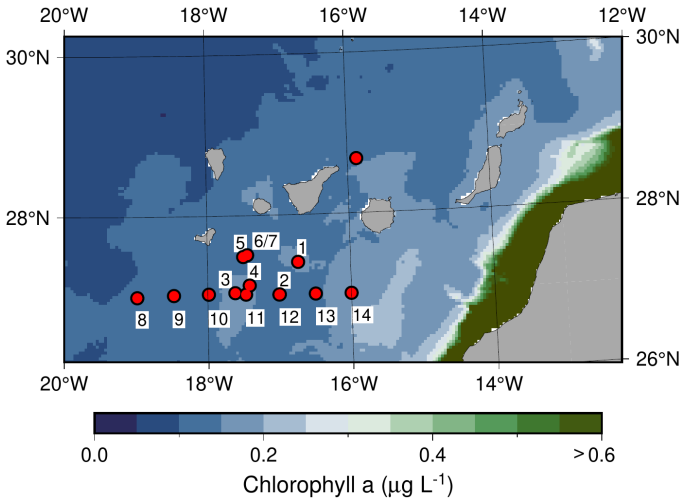

FIGURE 1
Map of the study area in the Canary Current. Red circles show the position of water sampling stations, and numbers show the locations of the 14 incubation experiments. Color shading shows monthly chlorophyll *a* in June 2022 from the Copernicus (CMEMS) GlobColour L4-satellite product.

Canary Islands also disturb the southward Canary Current and cause a relatively intense formation of meso-scale eddies that contribute to episodes with enhanced mixing with nutrient-rich deeper water (Valdés and Déniz-González, 2015). Eddy-induced mixing is therefore a significant contributor to primary production in the area (Sangrà et al., 2009). In addition, air-borne dust deposition from Africa occasionally contributes with minerals and trace metals to surface waters (Kandler et al., 2011).

2.2 Hydrography, turbulence and fluorescence

Measurements of conductivity (C), temperature (T) and pressure, i.e., depth (CTD), were measured with a loose-tethered free-fall Rockland Scientific International (RSI) VMP-250 microstructure vertical profiler in the upper 150-200 m. The profiler was equipped with a CT and pressure sensor (JFE

TABLE 1 Experiment number, station number, date and location for the incubation experiments with sample depth, concentration (1X = 0.061 g L^{-1}, 2X = 0.122 g L^{-1}) of the applied GRF and the sampling days for each experiment.

Experiments	Station no.	Date (YYMMDD)	Latitude (°N)	Longitude (°W)	Depth (m)	GRF-conc.	Sample days
Exp 1	1	220614	27°24.54'	16°43.97'	10	1xGRF	1, 3
Exp 2	2	220615	27°0.60'	16°49.96'	10	2xGRF	1, 6
Exp 3	3	220616	27°2.29'	17°37.95'	10	1xGRF	1, 6
Exp 4	4	220617	27°27.76'	17°24.88'	10	2xGRF	1, 4, 6
Exp 5	5	220618	27°29.19'	17°29.92'	114	1xGRF	4, 6
Exp 6	6	220619	27°29.97'	17°27.53'	90	2xGRF	4, 6
Exp 7	6	220619	27°29.97'	17°27.53'	10	1xGRF	4, 6
Exp 8	7	220620	27°0.95'	18°58.94'	90	1xGRF	4, 6
Exp 9	8	220621	27°0.95'	18°28.32'	110	2xGRF	4, 6
Exp 10	9	220622	27°1.47'	17°59.16'	10	1xGRF	4, 6
Exp 11	10	220623	27°1.50'	17°28.92'	10	1xGRF	4, 6
Exp 12	11	220624	27°0.05'	17°0.29'	10	1xGRF	4, 6
Exp 13	12	220625	27°0.40'	16°29.86'	10	1xGRF	2, 4
Exp 14	13	220626	27°0.13'	16°0.07'	87	1xGRF	2, 4
none	14	220629	28°40.57'	15°52.33'	–	–	–

Advantech) that operated at 16 Hz. Conservative temperature (Θ) and absolute salinity (S_A) was calculated according to TEOS-10 (IOC, 2010). In addition, the profiler was equipped with two shear sensors and a fluorescence sensor that operated at 64 Hz. Two casts were made at every station. The dissipation rate (ε) of turbulent kinetic energy was calculated with software provided by Rockland Scientific (Wolk et al., 2002; Lueck, 2016), and the vertical turbulent diffusion coefficient (k_v) was calculated as: $k_v = \Gamma\ \varepsilon/N^2$ (Osborn, 1980) where Γ is the mixing efficiency dependent on the ratio of ε/N^2 (Bouffard and Boegman, 2013; Bendtsen and Richardson, 2018) and N is the stratification frequency.

2.3 Water sampling, nutrients, light and chlorophyll *a*

Water samples were taken from standard depths (5, 10, 20, 40, 60, 100 m) and from the approximate depth of the deep chlorophyll *a* maximum (DCM) identified from the fluorescence profile mounted on the VMP-250 profiler. Water samples were collected using a 5 L Niskin bottle for measurements of nutrients and chlorophyll *a*, and by 2 x 10 L Niskin bottles at those depths where additional water was collected for incubations with GRF. The two 10 L Niskin bottles were closed simultaneously at the same depth. Niskin bottles were operated with a messenger, and a U-CTD probe (Ocean Science, Seabird CTD) was mounted below the Niskin bottle for precise measurements of pressure, temperature and conductivity at the sampling depth. Water samples for nutrients were tapped from the Niskin bottles and immediately frozen at -20°C. The samples were analyzed for nitrite, nitrate, ammonia, phosphorus (P) and silica (Si) by wet-chemistry methods (Grasshoff et al., 1983) with detection limits of 0.04, 0.1, 0.3, 0.06 and 0.2 µM, respectively. The analysis considered the total dissolved inorganic nitrogen-pool (DIN = $[NO_2^-]$ + $[NO_3^-]$ + $[NH_3^+]$) and changes in P were multiplied by 16 to represent the typical biological nutrient uptake rate of 16 moles of N for each mole of P (Redfield et al., 1963). Light measurements for photosynthetically available radiation (PAR) were made on deck (i.e., surface PAR) and inside the incubators with a ULM 500 (Waltz) data logger. PAR measurements in the upper 30 meters were measured with a spherical underwater quantum sensor (LI-193, LI-COR).

Chlorophyll *a* concentrations were measured from 1.5 L of seawater from selected sample depths (viz. 10 m and DCM) and 0.5 L from the incubation bottles and filtered through GF/F (pore size 0.7 µm, diameter 47 mm, Whatman) or GF5 (pore size 0.7 µm, diameter 47 mm, Chmlab) filters, and the filtration setup used a manifold (Pall Corporation). Folded filters were stored in tin foil and frozen at -20°C. Ethanol (96%) was used for extraction of chlorophyll. The extraction was conducted at 4°C and lasted 20 h. Measurements were performed by a fluorometer (Triology, Turner Design) which had been calibrated using a chlorophyll *a* standard (DHI, Hørsholm, Denmark).

2.4 Fv/Fm

The ratio of variable (Fv) and maximum (Fm) fluorescence was measured with a LabSTAF instrument (Chelsea Technologies Ltd; Oxborough, 2021) based on the method of fast repetition rate fluorometry (Kolber et al., 1998). Samples for Fv/Fm-measurements were stored immediately in darkness and measured after at least 30 min. All LabSTAF Fv/Fm-measurements were made in triplicates. A single turnover (ST) saturation phase was delivered with a 100-µs excitation pulse (452 nm) from the LabSTAF instrument to measure the minimum (Fo) and maximum (Fm) fluorescence (Boatman et al., 2019; Schuback et al., 2021). The quantum yield of photosystem II (PSII) was calculated as: Fv/Fm = (Fm-Fo)/Fm, where Fo is the minimum fluorescence from chlorophyll in a dark-adapted state. Fv/Fm is the quantum yield for a given photon flux and expresses the efficiency of the photosynthetic apparatus of transporting electrons (e.g., Gurbonov and Falkowski, 2022). Chlorophyll *a* in the incubation bottles was calculated from the maximum fluorescence (Fm) calibrated with a linear regression against chlorophyll *a* measurements from the incubation bottles: chlorophyll *a* = 1.132 Fm - 0.113 (n = 12, R^2 = 0.92; µg L^{-1}).

2.5 Incubations

Incubations were made on deck where three incubators (acrylic plastic, 2 x 175 L and 1 x 90 L) were temperature regulated by running surface water (Supplementary Figure S1). Incubation bottles (175 cm^2, polystyrene Sarstedt flasks) were free floating in the incubators such that wave motion kept the phytoplankton cells in suspension (Supplementary Figure S2). The temperature in the incubators was relatively constant throughout the cruise and varied between 22.5-24.3°C. Layers of Lagoon blue Lee LFTRN filters at the top and sides of the incubators reduced the light intensity by about a factor of 20. The photosynthetic available radiation (PAR) was measured regularly during the cruise and the average daylight in the incubators was 170 ± 90 µE m^{-2} s^{-1} (n = 66). The corresponding surface PAR was, on average, 3980 ± 1180 µE m^{-2} s^{-1} (n = 30). Water sampling was made around midday.

Incubations with GRF were made in ~650 ml culture flasks. Water was collected from the incubation depth in the 2 x 10 L simultaneously closed Niskin bottles and a coarse filter (200 µm) was applied for removing large zooplankton before the water was stored into 10 L containers on deck. Samples were divided into controls (CTL) and GRF-incubated bottles and placed in the incubators immediately after water collection. Control bottles with seawater were incubated without any further treatment, and GRF-incubations were prepared by dispersing dry glacial rock flour in 4 L of seawater before the incubation bottles were filled. Two concentrations of GRF were applied in the experiments with 0.061 ± 0.004 g L^{-1} and 0.122 ± 0.006 g L^{-1}, respectively (referred to as 1xGRF and 2xGRF, Table 1). Portions of GRF were measured by volume at sea and the weight was determined on land (n=10). The openings of the incubation bottles were sealed with Parafilm before random placement in the incubators. All treatments were made in triplicates and samples of CTL and GRF were measured in intervals of 1, 3, 4, and 6 days. The incubation bottles were removed after each measurement (e.g., treatments sampled after 4 and 6 days in Exp 5 implied 6 bottles

of both CTL and GRF to be incubated simultaneously, i.e., 12 bottles in total in Exp 5). Data analyses applied R (R Core Team, 2021) and the R-based BSDA-package of Welch modified two-sample t-test for the statistical analysis. The difference between treatments was referred to as significant when $p \leq 0.05$.

2.6 Glacial rock flour

The applied GRF was collected at a marine deposit in Ilulialik in the inner part of Godthåbsfjord located on the west coast of Greenland (Dietzen and Rosing, 2023). The GRF had originally been transported in a meltwater river originating from a land-terminated glacier from the Greenland Ice Sheet and deposited after the passage of a large lake (Tasersuaq) such that relatively fine-grained material (mica) reached the deposit (Sarkar, 2021). The applied GRF was similar to the material used in previous studies of terrestrial CO_2-sequestration (Dietzen and Rosing, 2023) and growth of crops (Gunnarsen et al., 2023). During the pre-processing of this material, the GRF was dried and stored in bags.

The composition of GRF was analyzed by Sarkar (2021). The median grain size (d_{50}) was 2.6 µm and with a relatively large BET-specific surface area of 19.6 m^2 g^{-1}. The mineral content of GRF consisted of mainly biotite (27.4%), oligoclase/andesine (18.6%), amphibole (14.6%), anorthite (14.1%), quartz (10.5%), Fe-oxide (2.8%), K-feldspar (2.8%), and muscovite (2.4%). Thus, GRF contains significant amounts of the macro nutrients silicate and phosphorus (but no nitrogen), and also essential trace metals such as iron and zinc that are limiting phytoplankton production in large areas of the ocean (e.g., Boyd and Ellwood, 2010). The extent to which these substances can be mobilized from GRF by marine organisms or become biologically accessible via chemical reactions with seawater (i.e., weathering) is unknown.

3 Results

3.1 Characteristics of the upper water mass

Sea surface temperature and salinity varied between 21-23°C and 37-37.4 g kg^{-1}, respectively (Figure 2A). The lowest surface salinities were observed at the easternmost station near the upwelling zone off Africa where salinities decreased to 36.6 g kg^{-1} (Figure 2A, dashed line). The North Atlantic Central Water mass (Θ < 18°C) occupied the depth range below the seasonal thermocline (~100 m). Mixed layer depths were in general 40-60 m deep (Figure 2B), and the largest dissipation

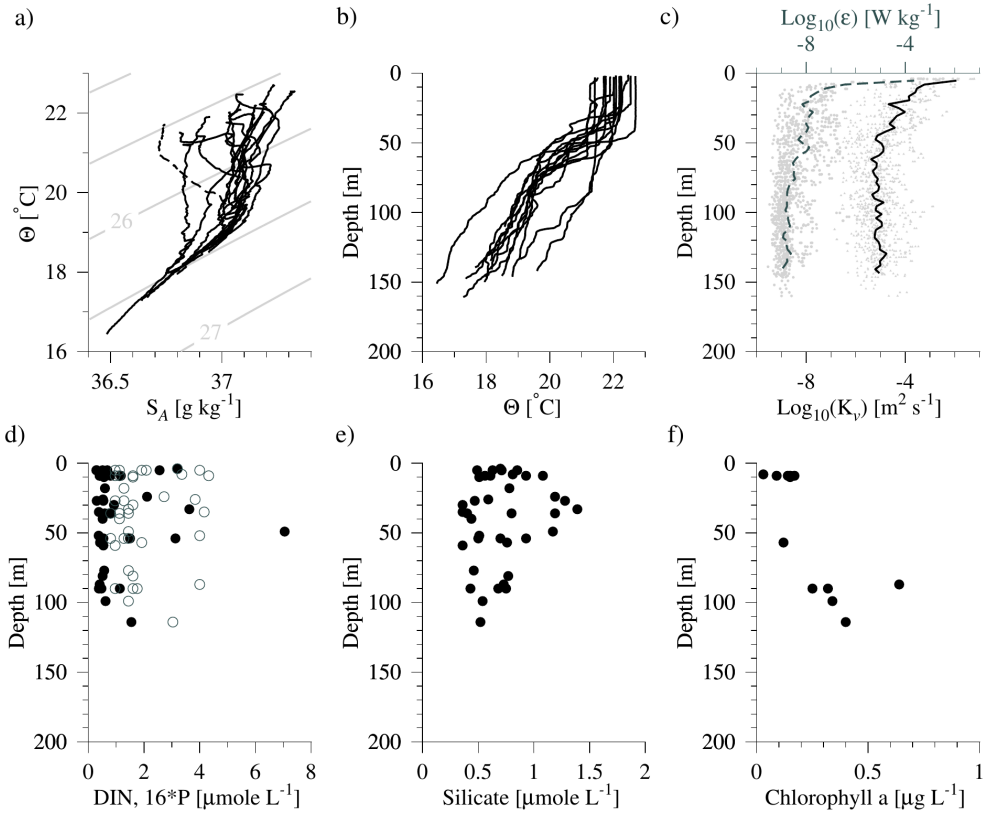

FIGURE 2
(A) Conservative temperature-absolute salinity diagram of vertical profiles from all experiments (isopycnals shown as contours). **(B)** Vertical profiles of conservative temperature, and **(C)** Log_{10} of dissipation rates of TKE and average profile (dashed line, data shown in light gray) and estimated vertical diffusion coefficients (full line, data in light gray). **(D)** Measurements of dissolved inorganic nitrogen (DIN, filled circles) and phosphorus multiplied with 16 (open circles), **(E)** silicate and, **(F)** chlorophyll *a*. The easternmost profile closest to the upwelling area off Africa is indicated by a dashed line in **A**.

rates of turbulent kinetic energy ($\varepsilon > 10^{-8}$ W kg^{-1}) and vertical turbulent diffusion coefficients ($k_v > 10^{-4}$ m^2 s^{-1}; i.e., a mixing time scale of a 10 m layer of less than a week) were seen in the mixed layer (Figure 2C). The diffusion coefficient was ~10^{-5} m^2 s^{-1} below the mixed layer, and this implied a relatively low vertical diffusive flux of heat, salinity and nutrients (i.e., a mixing time scale of a 10 m layer of > 100 days). Our data do not resolve the effects from short-time mixing events on biological productivity, e.g., due to wind, cooling at the surface or associated with meso-scale eddies (e.g., Richardson and Bendtsen, 2017).

In situ samples of DIN measured at a subset of stations were in general less than 2 µmole L^{-1} in the upper 100 m and a few samples had values between 2-8 µmole L^{-1}, likely due to eddy-induced mixing (Figure 2C; Supplementary Table S1). Comparison with the phosphorus concentration multiplied by 16 (16*P; Figure 2D, open circles) indicated that phytoplankton were limited by DIN rather than P, i.e., generally smaller DIN-values (filled circles in Figure 2D). Silicate measurements were also relatively low with typical values ~0.5 µmole L^{-1} and a few samples were above 1 µmole L^{-1} (Figure 2E). Chlorophyll *a* measurements were generally below 0.2 µg L^{-1} in the mixed layer and the highest concentration was less than 1 µg L^{-1} and observed below 80 m depth (Figure 2F). Thus, nutrients and chlorophyll *a* distributions showed that the area in general was nutrient-depleted and having a relatively low chlorophyll *a* concentration, except for a few stations likely influenced by eddy-mixing and supply of nutrients from below.

3.2 *In situ* light and variable fluorescence

Measurements of sub-surface PAR in the upper 25 m were made at stations for 5 experiments (Exp 4, 7, 9, 10, 13) in the afternoon with an average surface PAR of 4300 µE m^{-2} s^{-1}. In general, surface PAR during the day was ~4000 µE m^{-2} s^{-1} with a few periods with more dense cloud cover. The average light extinction in the upper 25 m was 0.038 ± 0.002 m^{-1} (n=5, SD), corresponding to an estimated euphotic depth (defined at the depth where light was 0.1% of the surface insolation) of 184 ± 12 m. Light levels at the incubation depths of 10 m and ~100 m were estimated to ~3000 and 110 µE m^{-2} s^{-1}, respectively. Thus, the light level in the incubators of ~170 µE m^{-2} s^{-1} during the day was significantly lower than light at 10 m depth, and comparable to deeper light levels in samples collected between 57-114 m depth.

Variable fluorescence Fv/Fm was also measured at the incubation depth levels at 10 m and ~100 m. However, Fv/Fm measurements were relatively low and at some samples from 10 m depth it was below detection. The average Fv/Fm at 10 m and ~100 m depth was 0.22 ± 0.06 (n = 9) and 0.32 ± 0.08 (n = 9), respectively. The low Fv/Fm-values near the surface and measurements of samples below the detection limit were likely due to photoinhibition due to the high light levels at 10 m depth around noon. Chlorophyll measurements (GF/F) at the 10 m and 100 m depth levels of 0.12 ± 0.05 (n = 5) and 0.35 ± 0.17 (n = 5), respectively, also indicated more optimal conditions for growth below the bottom of the mixed layer (Figure 2F).

3.3 Incubation changes in Fv/Fm and chlorophyll *a*

A significant increase of Fv/Fm was generally found in all experiments. In total, 25 comparisons were made between bottles incubated 1-6 days with and without GRF, and 18 of these showed a significantly ($p < 0.05$) higher Fv/Fm in the GRF-incubations (Figure 3; Supplementary Table S2). Only two of the comparisons (Exp 4 and 13) were significantly lower, and negative values were only seen at day one. Subsequent samples after 4 and 6 days showed that these two experiments also ended up with a significantly higher Fv/Fm in the GRF-incubations.

Similarly, differences in chlorophyll *a* showed a general increase in the GRF-incubated bottles where 13 of the 25 comparisons during the 6-day period showed a significantly ($p < 0.05$) higher chlorophyll *a* concentration (Figure 3B). Only two experiments showed a negative change, i.e., a higher concentration of chlorophyll *a* in the CTL-incubations: In one experiment (Exp 4) the chlorophyll *a* difference was only negative after the first day (cf., Fv/Fm in Figure 3A) and became significantly positive at the subsequent sampling days (days 4, 6), and in the other experiment (Exp 10) the negative chlorophyll difference was small.

In four experiments (Exp 2, 4, 6 and 9) the concentration of GRF was doubled (i.e., 2xGRF), and relatively high chlorophyll *a* concentrations in experiment 2, 4 and 9 indicated that this could be due to the higher GRF-concentration. This was supported by the significant ($p = 0.03$) different mean values after 6 days between experiments with the two different concentrations of GRF: 0.20 ± 0.06 µg L^{-1} (n = 7, 1xGRF) and 0.72 ± 0.26 µg L^{-1} (n = 4, 2xGRF), respectively.

The average response in Fv/Fm of all the incubations (Figure 4A) showed an increase of 0.04 ± 0.01 in GRF-bottles after 4 and 6 days (n = 9 and 11, respectively). In average the Fv/Fm increased in CTL-bottles from 0.32 ± 0.01 (n = 6) at day one to 0.34 ± 0.02 (n = 11) after six days (Figure 4B). This supported that the phytoplankton cells were functioning relatively well during the experiment, and that their conditions may even have improved. Thus, the experimental setup seemed not to influence their growth negatively. The increase in Fv/Fm of 0.04 in GRF- relative to CTL-bottles thereby corresponded to an increase of 12% in the photosynthetic quantum yield by the photosynthetic apparatus in the cells.

The average response in chlorophyll *a* (Figure 4C) showed a steady increase between the GRF- and CTL-bottles from 0.06 ± 0.04 µg L^{-1} (n = 6) at day one to an average difference of 0.39 ± 0.12 µg L^{-1} after 6 days (n = 11). The total concentration of chlorophyll *a* in the CTL-bottles showed a similar increase from a relatively low value of 0.07 ± 0.05 µg L^{-1} (n = 6) after the first day to 0.21 ± 0.07 µg L^{-1} (n = 11) after six days. The increased chlorophyll *a* concentrations during the 6 days were in accordance with the increased Fv/Fm, and also supported that the phytoplankton cells were not negatively influenced by the experimental treatment. The increased concentration of chlorophyll *a* also showed that phytoplankton was growing significantly during the 6-day period.

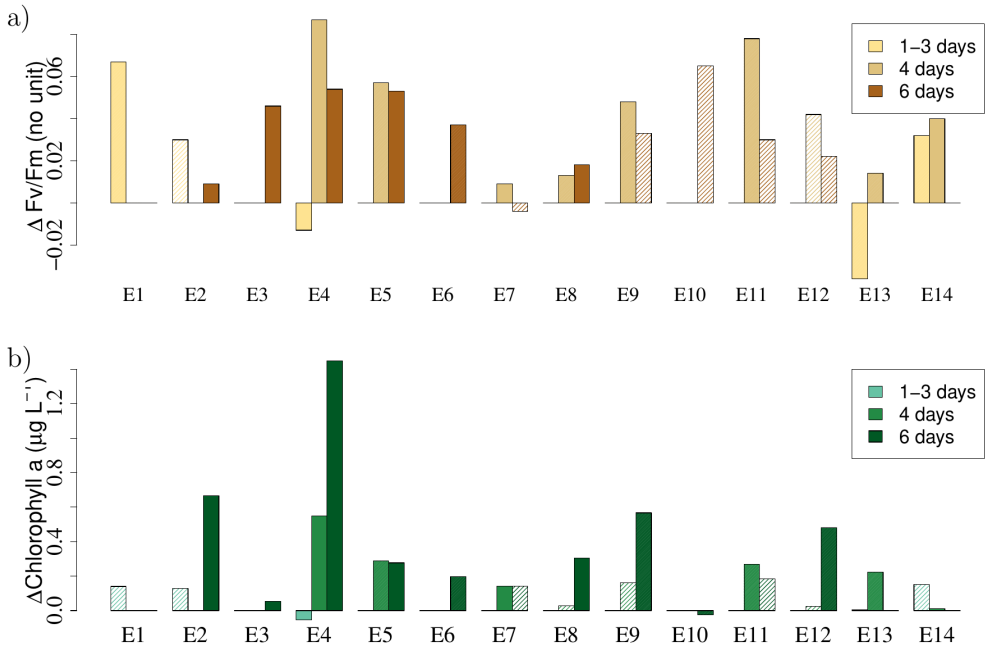

FIGURE 3
(A) Changes in Fv/Fm (ΔFv/Fm) in the 14 experiments (E1-E14) between incubations with GRF and without GRF (i.e., GRF-CTL), and **(B)** the corresponding difference in chlorophyll *a* (ΔChlorophyll *a*). Differences are calculated from average values of triplicates sampled after 1-3, 4 and 6 days. Significant (t-test, $p < 0.05$) differences are shown with filled colors and non-significant differences are shown in shaded colors.

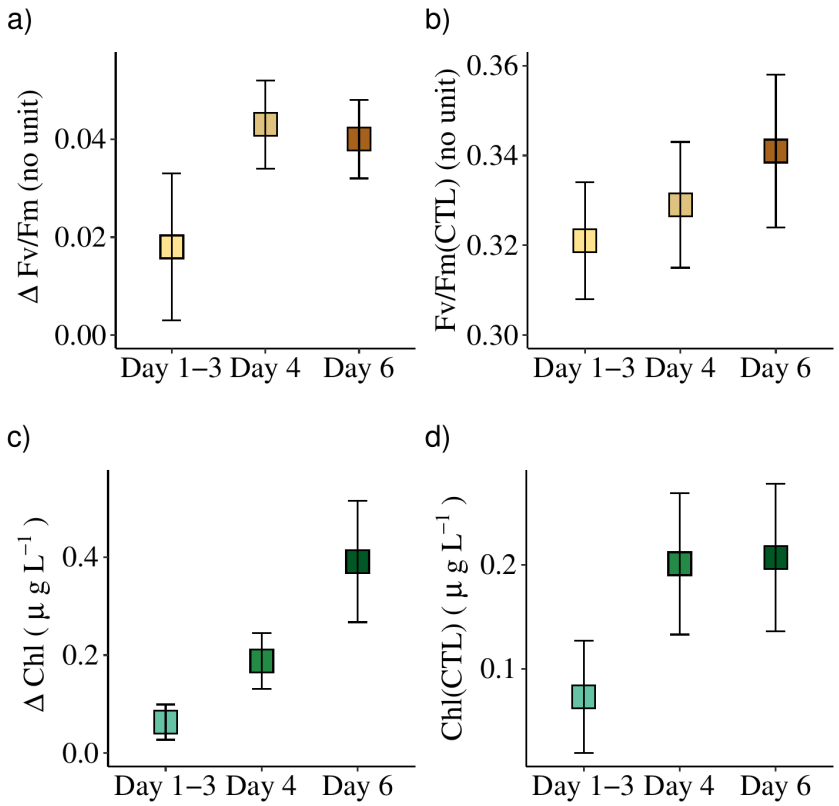

FIGURE 4
(A) Average changes (± SE) from all incubations sampled after 1-3, 4 and 6 days in Fv/Fm (ΔFv/Fm) between incubations with and without GRF, i.e., GRF-CTL, and **(C)** the corresponding changes in chlorophyll *a* (ΔChl). The average values of the CTL-bottles are shown for Fv/Fm **(B)** and chlorophyll *a* **(D)**.

3.4 Incubation changes in nutrients

Changes in dissolved phosphorus (P), silicate (Si) and inorganic nitrogen (DIN) between the GRF- and CTL-bottles after 6 days were related to the potential photosynthetic uptake or remineralization of organic matter, e.g., pools of dissolved and particulate organic matter in the water samples (Figure 5; Supplementary Table S2). Changes in P were therefore multiplied by 16 in the analysis. In general, there was a larger negative change of P in the GRF-bottles where 8 out of 14 comparisons were significantly lower and none had a positive change, i.e., the GRF-bottles had a larger P-consumption. In contrast, the Si-concentration generally increased in the GRF-bottles where 6 experiments ended up with a significantly larger Si-concentration than the CTL-bottles, whereas only 3 experiments had a negative change in silicate. The change of DIN varied between significant positive (n = 6) and negative (n = 6) changes between the GRF- and CTL-bottles. In general, the variation of concentration changes between the three compounds were comparable.

The average response in nutrients (ΔNutrients) after six days showed that GRF-bottles contained 0.06 ± 0.01 µmole L^{-1} (n = 13) less P than the CTL-bottles, i.e., corresponding to a 16*ΔP of -1.0 µmole L^{-1} (Figure 6A). The corresponding change in Si and DIN showed a higher concentration in the GRF-bottles of ΔSi = 0.25 ± 0.11 µmole L^{-1} and ΔDIN = 0.11 ± 0.23 µmole L^{-1}, respectively. Thus, the change in the three nutrient pools did not co-vary which showed that other processes than biological uptake due to photosynthesis were involved in changing the nutrient concentration between the GRF- and CTL-bottles.

The average concentration of P in the CTL-bottles after six days of 0.09 ± 0.02 µmole L^{-1} (Figure 6B) was slightly larger than the average initial concentration of 0.08 ± 0.02 µmole L^{-1}. This indicated that additional P had been remineralized from the organic pools and contributed to both the increased P-concentration of ~0.01 µmole L^{-1} and the increased biomass (Figure 4D). Similarly, the concentration of Si and DIN increased by 0.03 and 0.78 µmole L^{-1}, respectively. Thus, the average nutrient concentrations showed that the CTL-bottles had a higher concentration of nutrients after six days than the initial concentrations, and this could be explained by a significant microbial remineralisation of organic matter taking place during the 6-day period. The average change between the GRF- and CTL-bottles (Figure 6A) showed that additional Si and DIN was supplied in the GRF-bottles whereas a significantly larger average P-consumption was taking place here. These differences are discussed further below.

4 Discussion

Application of GRF as source material for mCDR via increasing ocean biological production and subsequent carbon-storage by export (i.e., sinking and mixing) of organic matter into the ocean interior implies several steps and processes to be considered in the oceanic carbon cycle. The first step involves CO_2-uptake associated with photosynthetic production of organic matter. The next step is to enhance export of the organic matter bound carbon to the deep-sea to avoid subsequent remineralisation of the organic matter near the surface. This may lead to only a short-term sequestration and return of CO_2 to the atmosphere. This study focuses on the first step, i.e., the potential for increasing primary production by phytoplankton. Before any substances are applied in an mCDR-technology there are indeed additional issues to consider; the impacts on marine ecosystems and nutrient cycling, e.g., promoting certain phytoplankton species by their dependencies on Si or Fe (e.g., Bach et al., 2019), time-scales for the ocean carbon-storage (e.g., Aumont and Bopp, 2006; Keller et al., 2014), assessment of the environmental impact associated with exploitation of the applied substance, and also for the economic or commercial feasibility of the method. These aspects are not covered in detail here, and are subjects for further studies applying GRF as a potential means of action for mCDR.

4.1 Supply of trace metals from GRF

GRF-incubations showed that Fv/Fm increased significantly after 4-6 days, and a similar increase was observed in the concentration of chlorophyll *a* (Figure 4). Thus, both photosynthetic activity and phytoplankton growth were enhanced

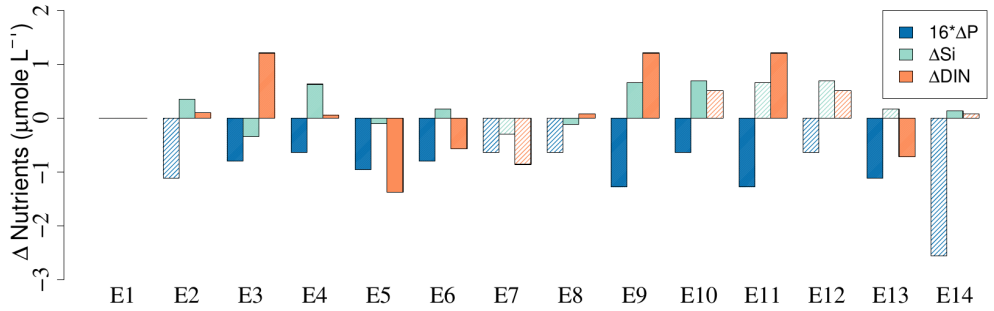

FIGURE 5
Changes in phosphorus multiplied with 16 (16*ΔP), silicate (ΔSi) and DIN (ΔDIN) in the 14 experiments between incubations with GRF and without GRF (i.e., GRF-CTL). Differences are calculated from average values sampled at the end of the experiments, i.e., after 4 days or 6 days (Table 1). Significant (t-test, $p < 0.05$) differences are shown with filled colors and non-significant differences are shown in shaded colors.

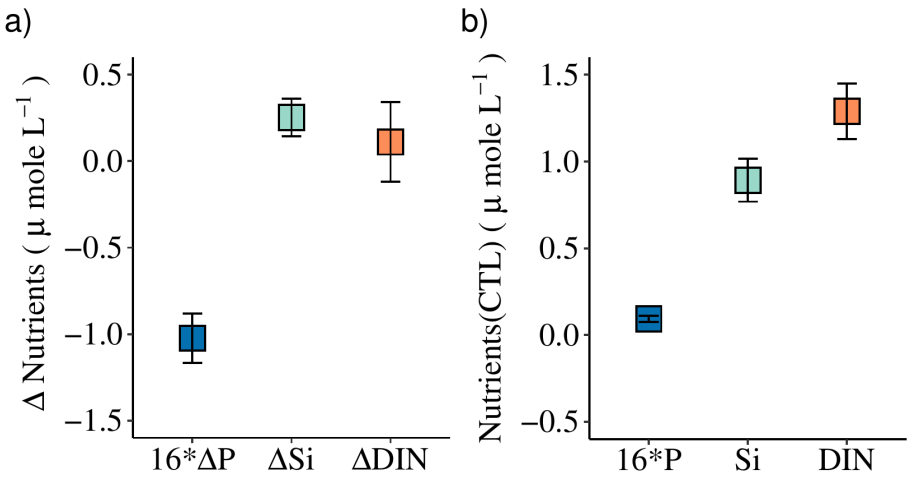

FIGURE 6
(A) Average changes (± SE) in the end of the experiments from all incubations samples after 4 and 6 days in phosphorous multiplied with 16 (Δ16*P), silicate (ΔSi) and DIN (ΔDIN), between incubations with and without GRF, i.e., GRF-CTL. **(B)** The average nutrient concentration in the CTL-bottles.

by GRF. Four of the 14 experiments applied a doubling of the GRF-concentrations, and showed a significantly larger chlorophyll *a* concentration when compared with the other experiments. This indicates that increasing GRF-concentrations stimulate phytoplankton growth further.

We suggest that the main stimulus from GRF on phytoplankton growth is due to its supply of nutrients and trace metals. The average mineral composition of GRF included macro-nutrients as silicate (i.e., ~54% SiO_2, g/100 g) and phosphorus (0.01 ppm P_2O_5 and 0.43 ppm PF). Iron was the largest trace metal compound (0.86 ppm Fe_2O_3) (Sarkar, 2021; Dietzen and Rosing, 2023). The corresponding concentrations of the suspended GRF-material in the 1xGRF (0.06 g L^{-1}) experiments corresponded to 36, 0.05 and 0.03 mmol L^{-1} of Si, P and Fe, respectively. The nutrient requirement for phytoplankton growth in the GRF-incubations were estimated from the average chlorophyll *a* increase of ~0.5 µg L^{-1} (Figure 4). We presume an organic carbon:chlorophyll *a* ratio ~40 in the phytoplankton cells, i.e., within the observed range (e.g., Sathyendranath et al., 2009). This implies a particulate organic carbon pool of ~2 µmole Carbon L^{-1}. Thus, the total nutrient and trace metal content in the suspended GRF of these three substances was much greater than the requirement for explaining the observed phytoplankton growth, although only a fraction of the GRF dissolves via chemical weathering or otherwise becomes biologically available during the 6-day incubation period (coarse grains and suspended material were visible in the bottles at the end of the incubations). Hence, the total mineral content shows that GRF has the potential to support significant growth by supplying Si, P and Fe. In general, the initial concentration of DIN, Si and P showed that the average ratios DIN/P (6.1) and Si/DIN (16.8) from all the experiments (Supplementary Table S1) indicated that the phytoplankton was mainly limited by DIN, although a single experiment (Exp 5) had a relatively low Si concentration (Si/DIN = 0.3), and another experiment showed potential P-limitation (i.e., DIN/P~20 in Exp 3). The concentration of macronutrients therefore, in general, indicated that nitrogen was the limiting factor for phytoplankton growth, in accordance with previous findings from the area (Cianca et al., 2007; Valdés and Déniz-González, 2015). The GRF did not contain nitrogen compounds (other nitrogen sources are discussed in Section 4.2), and therefore we suggest that the major stimuli for phytoplankton growth was the supply of trace metals. The consumption of Fe is relatively low in phytoplankton cells (i.e., C:Fe ratios >1000, Twining and Baines, 2013) and the iron-content in GRF can therefore be a potential iron-source. There is a continuous transfer of dissolved reduced Fe (II) into the colloidal iron-pool in oxygenated seawater (de Baar et al., 2005), and the relatively high Fe-concentration in GRF therefore makes it a likely supply of dissolved iron for further growth. In addition, GRF contains a suite of other substances, particularly other essential trace metals for phytoplankton growth (Twining and Baines, 2013) as Zn (>100 ppm bw.), Mn (i.e., MnO~1 ppm), Ni (~130 ppm), Cu (~80 ppm) and also essential substances that only is required in tiny amounts as Co (~30 ppm), Cd (~0.1 ppm), and Mo (~1 ppm) (Sarkar, 2021; Dietzen and Rosing, 2023). In summary, increased growth and photosynthetic activity in the GRF-incubations was likely stimulated by trace metals biologically mobilized or weathered from the GRF, and in particular the supply of iron, i.e., an essential trace metal in the functioning of the photosynthetic apparatus (e.g., Gorbunov and Falkowski, 2022), may explain the increased photosynthetic activity and increase in chlorophyll *a*.

4.2 Weathering and nutrients from remineralisation

In general, the upper water masses were nutrient-limited with relatively low *in situ* concentrations of DIN, Si and P. Vertical turbulent fluxes of nutrients were relatively small below the mixed layer. This indicated that nutrient cycling in the upper ~100 m mainly was supplied by recycling of remineralized organic matter. This is in accordance with the conceptual cycling of organic matter

in the area where the high-productive upwelling zone off Africa supplies sub-surface water masses in the Canary Current with organic matter (Valdés and Déniz-González, 2015). The presence of organic matter (e.g., dissolved or particulate organic nitrogen) in the water samples could explain the relatively modest increase of DIN in the GRF-incubations. Increased microbial remineralisation of the pool of labile organic matter in the open ocean generally takes place on a time-scale of about a week (Bendtsen et al., 2015) and microbial remineralisation of organic matter could therefore cause the observed increase of DIN and, thereby, also DIC. Remineralisation of organic matter would counteract the influence on surface pCO_2 from the removal of DIC by phytoplankton growth. Zubkov et al. (2007) found that bacterioplankton (for example the photosynthetic prokaryote *Prochlorococcus*) dominated the uptake of bioavailable phosphorus in the North Atlantic subtropical gyre and such microbial processes could also explain the general decoupling of N- and P-uptake in the incubations. Similar decoupling was also noted in the alkalinity-enhancement study of Subhas et al. (2022) in incubations with surface water from the central and western subtropical Atlantic.

This aspect of stimulating the bacterial community with GRF have to be considered before GRF is applied for mCDR. However, the average increase of 0.11 µmole DIN L^{-1} in the GRF-incubations was about a factor of 10 less than the corresponding carbon uptake implied by the decrease in P (i.e., 16*ΔP = -1.0 µmole L^{-1}). Thus, assuming that the DIC: DIN:P ratio from remineralized organic matter can be represented by Redfield molar ratios (106:16:1), the resultant net effect from the supply of GRF would be to remove 10 times more DIC than would be associated with the DIC remineralized from the pool of organic matter. In addition, the excess pool of remineralized DIN would also be expected to be consumed by phytoplankton on longer time scales (~weeks), and thereby the counteracting effect on CO_2-sequestration would disappear.

A relatively high increased concentration of silicate (0.25 µmole L^{-1}) was seen in the GRF-incubations, and this could be explained by either dissolution of silicate from diatoms or other silicate-containing organism or, more likely, due to weathering of silicate from GRF. Weathering of silicate minerals implies an increase in surface alkalinity from the associated increase of conservative cat-ions, and this results in a decrease of pCO_2. Thus, the GRF-incubations indicate that significant silicate weathering takes place during the relatively short period. This alkalinization would tend to increase the oceanic CO_2-uptake further, and thereby increase the CO_2-sequestration from GRF.

4.3 GRF and carbon-export

A critical process for mCDR-technologies to work *in situ* is the resultant carbon export into the ocean interior and this aspect is presently poorly understood. Aggregate formation is a key process that transforms small organic particles into fast sinking aggregates, i.e., marine snow (Alldredge and Silver, 1988; Jackson, 1990). Thus, aggregation of GRF together with particulate organic carbon (e.g., detritus or phytoplankton cells) could drive a fast carbon export similar to observations of sinking organic matter associated with surface deposition of Saharan dust (e.g., Báez-Hernández et al., 2019). Inorganic particles prime aggregate formation (Honjo and Farrington, 1982) and as part of the aggregate matrices, silt and clay particles act as ballast and the fast-sinking aggregates scavenge and incorporate even more organic material during their sinking through the water column (Hansen et al., 1996). However, increased sinking velocities of the dispersed GRF could also mean incomplete weathering due to a shorter residence time of GRF in the surface waters such that its full potential for CO_2-sequestration is not achieved. Observations show that C:N-ratios in particulate organic matter can be larger than Redfield ratios (e.g., Bendtsen et al., 2015) and this would tend to further increase the amount of carbon per mole of nitrogen uptake. Thus, more knowledge of these aspects of large-scale applications of GRF for mCDR are required.

4.4 Application of GRF for mCDR

Scaling up marine CO_2 removal to become a significant global carbon sink implies exploitation of source material at a scale similar to other global industries, e.g., cement-production. GRF originates below the Greenland Ice Sheet and has accumulated since the last glacial period in sedimentary deposits as fine-grained silt (Bennike et al., 2019). The material is therefore relatively easy to access and available in large amounts with the potential to remove CO_2 at the level of gigatonnes. The natural formation process of GRF results in a small grain size. Energy is therefore not necessary for further crushing and grinding of the material that would otherwise reduce the net sequestration potential of the rock material (Hangx and Spiers, 2009).

Distribution at the ocean surface of a source material for mCDR could be carried out with a fleet of dedicated vessels or combined with commercial container traffic at sea (NASEM, 2021). A similar approach could also be the basis for distributing GRF. This study (though small in scale) shows the positive effect from GRF on phytoplankton growth. However, there is also a need for a more comprehensive understanding of how a possible change in the phytoplankton community composition may impact higher trophic levels. The significant photosynthetic response and associated growth in the nutrient depleted waters in the Canary Current indicated that nutrients and trace metals from GRF can be mobilized on a weekly time scale. This makes promise of an even larger response in nutrient replete but trace metal limited ocean areas, e.g., the Southern Ocean, the subpolar North Pacific or the subpolar North Atlantic. Those areas would be relevant for further studies of ecosystem response to supplies of GRF.

5 Conclusion

The impact of glacial rock flour (GRF) on phytoplankton growth was investigated in 14 incubation experiments carried out with natural phytoplankton communities in the subtropical North Atlantic. Specifically, the incubations were based on water samples

collected from the upper 100 m in the Canary Current. The incubated phytoplankton communities were therefore representative of the open ocean. Bottles with and without GRF were compared during a 6-day period where light and temperature were regulated in incubators on the deck. In general, bottles incubated with GRF had a significantly higher variable fluorescence, and on average, this corresponded to a 12% increase in the photosynthetic quantum yield. The average response of chlorophyll *a* also showed a steady increase during the 6 days. These findings showed that the supply of GRF stimulated phytoplankton growth significantly in comparison with control experiments. We suggest that trace metals (e.g., Fe) in the fine-grained multi-composite GRF-material, become mobilized during the incubations and supply the cells with these essential elements. Thus, supply of GRF has the potential to increase photosynthetic activity and biological production. GRF is a large resource that is naturally supplied to the ocean via rivers around Greenland, and relatively easily accessible for exploitation. Supply of GRF in trace metal limited ocean areas could potentially lead to a significant increase in biological production and oceanic CO_2-uptake. These results motivate further studies on the chemical and biological mobilization of trace metals and nutrients from GRF, as well as the impact it may have on other aspects of the ocean carbon cycle, e.g., ecosystems in the entire water column and alkalinization of the surface water. Thus, GRF could be considered as a means of action for marine carbon dioxide removal (mCDR).

Data availability statement

The original contributions presented in the study are included in the article/Supplementary Material. Further inquiries can be directed to the corresponding author.

Author contributions

JB: Writing – original draft, Writing – review & editing. ND: Writing – original draft, Writing – review & editing. JH: Writing – original draft, Writing – review & editing.

Funding

The author(s) declare financial support was received for the research, authorship, and/or publication of this article. The cruise was supported by funding from the Microsoft Foundation. JB was supported by the NOVO Nordisk foundation (NNF22SA0079616).

Acknowledgments

We thank the captain and crew on-board the schooner Activ for helpful assistance and support during the cruise. We thank the Carlsberg Foundation for equipment grants (2013_01_0259, CF15-0301 and CF19-0051). The Glob-Colour chlorophyll *a* L4-satellite product, was generated using CMEMS Products, production center ACRI-ST.

Conflict of interest

The authors declare that the research was conducted in the absence of any commercial or financial relationships that could be construed as a potential conflict of interest.

Publisher's note

Supplementary material

The Supplementary Material for this article can be found online at: https://www.frontiersin.org/articles/10.3389/fmars.2024.1416421/full#supplementary-material

References

Alldredge, A. L., and Silver, M. W. (1988). Characteristics, dynamics and significance of marine snow. *Progr. Oceanogr.* 20, 41–82. doi: 10.1016/0079-6611(88)90053-5

Andresen, C. S., Karlsson, N. B., Straneo, F., Schmidt, S., Andersen, T. J., Eidam, E. F., et al. (20241332). Sediment discharge from Greenland's marine-terminating glaciers is linked with surface melt. *Nat. Commun.* 15, 1332. doi: 10.1038/s41467-024-45694-1

Aumont, O., and Bopp, L. (2006). Globalizing results from ocean in *situ* iron fertilization studies. *Global Biogeochem. Cycles* 20, GB2017. doi: 10.1029/2005GB002591

Bach, L. T., Gill, S. J., Rickaby, R. E. M., Gore, S., and Renforth, P. (2019). CO_2 removal with enhanced weathering and ocean alkalinity enhancement: potential risks and co-benefits for marine pelagic ecosystems. *Front. Climate* 1. doi: 10.3389/fclim.2019.00007

Báez-Hernández, M., García, N., Menéndez, I., Jaramillo, A., Sánchez-Pérez, I., and Santana, Á (2019). Interaction of sinking behavior of Saharan dust and lithogenic and biogenic fluxes in the Canary Basin. *Sci. Mar.* 83, 121–132. doi: 10.3989/scimar.04877.19A

Bendtsen, J., Hilligsøe, K. M., Hansen, J. L. S., and Richardson, K. (2015). Analysis of remineralisation, lability, temperature sensitivity and structural composition of organic matter from the upper ocean. *Prog. Oceanogr.* 130, 125–145. doi: 10.1016/j.pocean.2014.10.009

Bendtsen, J., and Richardson, K. (2018). Turbulence measurements suggest high rates of new production over the shelf edge in the northeastern North Sea during summer. *Biogeosciences* 15, 7315–7332. doi: 10.5194/bg-15-7315-2018

Bennike, O., Jensen, J. B., Sukstorf, F. N., and Rosing, M. T. (2019). Mapping glacial rock flour deposits in Tasersuaq, Southern West Greenland. *Geol. Surv. Den. Greenl. Bull.* 43, 1–5. doi: 10.34194/GEUSB-201943-02-06

Boatman, T. G., Geider, R. J., and Oxborough, K. (2019). Improving the accuracy of single turnover active fluorometry (STAF) for the estimation of phytoplankton primary productivity (PhytoPP). *Front. Mar. Sci.* 6. doi: 10.3389/fmars.2019.00319

Bouffard, D., and Boegman, L. (2013). A diapycnal diffusivity model for stratified environmental flows. *Dyn. Atmos. Oceans.* 61–62, 14–34. doi: 10.1016/j.dynatmoce.2013.02.002

Boyd, P., and Ellwood, M. (2010). The biogeochemical cycle of iron in the ocean. *Nat. Geosci.* 3, 675–682. doi: 10.1038/ngeo964

Boyd, P. W., Jickells, T., Law, C. S., Blain, S., Boyle, E. A., Buesseler, K. O., et al. (2007). Mesoscale iron enrichment experiments 1993-2005: Synthesis and future directions. *Science* 315, 612–617. doi: 10.1126/science.1131669

Canadell, J. G., Monteiro, P. M. S., Costa, M. H., Cotrim da Cunha, L., Cox, P. M., Eliseev, A. V., et al. (2021). "Global carbon and other biogeochemical cycles and feedbacks. In climate change 2021: the physical science basis," in *Contribution of working group I to the sixth assessment report of the intergovernmental panel on climate change*. Eds. V. Masson-Delmotte, P. Zhai, A. Pirani, S. L. Connors, C. Péan, S. Berger, et al (Cambridge University Press, Cambridge, United Kingdom and New York, NY, USA), 673–816. doi: 10.1017/9781009157896.007

Cianca, A., Helmke, P., Mourinō, B., Rueda, M. J., Llinas, O., and Neuer, S. (2007). Decadal analysis of hydrography and in *situ* nutrient budgets in the western and eastern North Atlantic subtropical gyre. *J. Geophys. Res.* 112, C07025. doi: 10.1029/2006JC003788

de Baar, H. J. W., Boyd, P. W., Coale, K. H., Landry, M. R., Tsuda, A., Assmy, P., et al. (2005). Synthesis of iron fertilization experiments: From the Iron Age in the Age of Enlightenment. *J. Geophys. Res.* 110, C09S16. doi: 10.1029/2004JC002601

Dietzen, C., and Rosing, M. T. (2023). Quantification of CO_2 uptake by enhanced weathering of silicate minerals applied to acidic soils. *Int. J. Greenhouse Gas Control* 125, 103872. doi: 10.1016/j.ijggc.2023.103872

Gorbunov, M. Y., and Falkowski, P. G. (2022). Using chlorophyll fluorescence to determine the fate of photons absorbed by phytoplankton in the world's oceans. *Annu. Rev. Mar. Sci.* 14, 213–238. doi: 10.1146/annurev-marine-032621-122346

Grasshoff, K., Ehrhardt, M., and Kremling, K. (1983). *Methods of seawater analysis, 2nd edn* (Weinheim: Verlag Chemie).

Gunnarsen, K. C., Jensen, L. S., Rosing, M. T., and Dietzen, C. (2023). Greenlandic glacial rock flour improves crop yield in organic agricultural production. *Nutr. Cycl. Agroecosyst.* 126, 51–66. doi: 10.1007/s10705-023-10274-0

Hangx, S. J. T., and Spiers, C. J. (2009). Coastal spreading of olivine to control atmospheric CO_2 concentrations: A critical analysis of viability. *Int. J. Greenhouse Gas Control* 3, 757–767. doi: 10.1016/j.ijggc.2009.07.001

Hansen, J. L. S., Kiørboe, T., and Alldredge, A. L. (1996). Marine snow derived from abandoned larvacean houses: sinking rates, particle content and mechanisms of aggregate formation. *Mar. Ecol. Progr. Ser.* 141, 205–215. doi: 10.3354/meps141205

Honjo, S., and Farrington, J. W. (1982). Deep advective transport of lithogenic particles in Panama basin. *Science* 216, 516–518. doi: 10.1126/science.216.4545.516

IOC, SCOR and IAPSO (2010). *The international thermodynamic equation of seawater–2010: Calculation and use of thermodynamic properties. Intergovernmental Oceanographic Commission, Manuals and Guides No. 56, UNESCO (English).* 196.

IPCC (2018). *Global Warming of 1.5°C. An IPCC Special Report on the impacts of global warming of 1.5°C above pre-industrial levels and related global greenhouse gas emission pathways, in the context of strengthening the global response to the threat of climate change, sustainable development, and efforts to eradicate poverty*. Eds. Masson-Delmotte, V., Zhai, P., Pörtner, H.-O., Roberts, D., Skea, J., Shukla, P. R., et al.

Jackson, G. A. (1990). A model of the formation of marine algal flocs by physical coagulation processes. *Deep-Sea Res.* 37, 1197–1211. doi: 10.1016/0198-0149(90)90038-W

Jørgensen, C. J., Søndergaard, J., Larsen, M. M., Kjeldsen, K. K., Rosa, D., Sapper, S. E., et al. (2024) Large mercury release from the Greenland Ice Sheet invalidated. *Sci. Adv.* 10, eadi7760. doi: 10.1126/sciadv.adi7760

Kandler, K., Schütz, L., Jäckel, S., Lieke, K., Emmel, C., Müller-Ebert, D., et al. (2011). Ground-based off-line aerosol measurements at Praia, Cape Verde, during the Saharan Mineral Dust Experiment: Microphysical properties and mineralogy. *Tellus Ser. B* 63, 459–474. doi: 10.1111/j.1600-0889.2011.00546.x

Keller, D., Feng, E., and Oschlies, A. (2014). Potential climate engineering effectiveness and side effects during a high carbon dioxide-emission scenario. *Nat. Commun.* 5, 3304. doi: 10.1038/ncomms4304

Kolber, Z. S., Prášil, O., and Falkowski, P. G. (1998). Measurements of variable chlorophyll fluorescence using fast repetition rate techniques: defining methodology and experimental protocols. *Biochim. Biophys. Acta* 1367, 88–106. doi: 10.1016/s0005-2728(98)00135-2

Lueck, R. (2016). *Calculating the rate of dissipation of turbulent kinetic energy, RSI Technical Note 028, Rockland Scientific International* (Victoria, Canada:Rockland Scientific International), 18.

Mills, M. M., Ridame, C., Davey, M., La Roche, J., and Geider, J. (2004). Iron and phosphorous co-limit nitrogen fixation in the eastern tropical North Atlantic. *Nature* 429, 292–294. doi: 10.1038/nature02550

NASEM and National Academies of Sciences, Engineering, and Medicine (2021). *A research strategy for ocean-based carbon dioxide removal and sequestration* (Washington, DC: The National Academies Press). doi: 10.17226/26278

Osborn, T. R. (1980). Estimate of the local rate of vertical diffusion from dissipation measurements. *J. Phys. Oceanogr.* 10, 83–89. doi: 10.1175/1520-0485(1980)010<0083:EOTLRO>2.0.CO;2

Overeem, I., Hudson, B., Syvitski, J., Mikkelsen, A. B., Hasholt, B., van den Broeke, M. R., et al. (2017). Substantial export of suspended sediment to the global oceans from glacial erosion in Greenland. *Nat. Geosci.* 10, 859–863. doi: 10.1038/ngeo3046

Oxborough, K. (2021). *LabSTAF and runSTAF handbook: 2408-014-HB | Issue E. West molesey, UK, chelsea technologies ltd.* 116, (Doc No. 2408-014-HB | Issue E). doi: 10.25607/OBP-1029.3

Paris Agreement to the United Nations Framework Convention on Climate Change (2015). T.I.A.S. No. 16-1104.

R Core Team (2021). *R: A language and environment for statistical computing* (Vienna, Austria: R Foundation for Statistical Computing). Available at: https://www.R-project.org/.

Redfield, A. C., Ketchum, B. H., and Richards, F. A. (1963). The influence of organisms on the composition of sea water. *In: Hill M.N. (Ed.) Sea. Wiley-Interscience New York* pp, 26–77.

Richardson, K., and Bendtsen, J. (2017). Photosynthetic oxygen production in a warmer ocean: the Sargasso Sea as a case study. *Phil. Trans. R. Soc A* 375, 20160329. doi: 10.1098/rsta.2016.0329

Sangrà, P., Pascual, A., Rodríguez-Santana, Á., Machín, F., Mason, E., McWilliams, J. C., et al. (2009). The Canary Eddy Corridor: A major pathway for long-lived eddies in the subtropical North Atlantic. *Deep Sea Res.* 56, 2000–2014. doi: 10.1016/j.dsr.2009.08.008

Sarkar, S. R. (2021). *Glacial Rock Flour: Its characteristic and enhanced weathering* (Denmark:University of Copenhagen (PhD Thesis)).

Sathyendranath, S., Stuart, V., Nair, A., Oka, K., Nakane, T., Bouman, H., et al. (2009). Carbon-to-chlorophyll ratio and growth rate of phytoplankton in the sea. *Mar. Ecol. Prog. Ser.* 383, 73–84. doi: 10.3354/meps07998

Schuback, N., Tortell, P. D., Berman-Frank, I., Campbell, D. A., Ciotti, A., Courtecuisse, E., et al. (2021). Single-turnover variable chlorophyll fluorescence as a tool for assessing phytoplankton photosynthesis and primary productivity: opportunities, caveats and recommendations. *Front. Mar. Sci.* 8. doi: 10.3389/fmars.2021.690607

Subhas, A. V., Marx, L., Reynolds, S., Flohr, A., Mawji, E. W., Brown, P. J., et al. (2022). Microbial ecosystem responses to alkalinity enhancement in the North Atlantic Subtropical Gyre. *Front. Clim.* 4. doi: 10.3389/fclim.2022.784997

Twining, B. S., and Baines, S. B. (2013). The trace metal composition of marine phytoplankton. *Annu. Rev. Mar. Sci.* 5, 191–215. doi: 10.1146/annurev-marine-121211-172322

Valdés, L., and Déniz-González, I. (2015). *Oceanographic and biological features in the Canary Current Large Marine Ecosystem* Vol. 115 (IOC-UNESCO, Paris: IOC Technical Series), 383.

Wolk, F., Yamazaki, H., Seuront, L., and Lueck, R. G. (2002). A new free-fall profiler for measuring bio-physical microstructure. *J. Atmos. Ocean. Tech.* 19, 780–793. doi: 10.1175/1520-0426(2002)019<0780:ANFFPF>2.0.CO;2

Yoon, J.-E., Yoo, K.-C., Macdonald, A. M., Yoon, H.-I., Park, K.-T., Yang, E. J., et al. (2018). Reviews and syntheses: Ocean iron fertilization experiments—past, present, and future looking to a future Korean Iron Fertilization Experiment in the Southern Ocean (KIFES) project. *Biogeosciences* 15, 5847–5889. doi: 10.5194/bg-15-5847-2018

Zubkov, M. V., Mary, I., Woodward, E. M. S., Warwick, P. E., Fuchs, B. M., Scanlan, D. J., et al. (2007). Microbial control of phosphate in the nutrient-depleted North Atlantic subtropical gyre. *Environ. Microbiol.* 9, 2079–2089. doi: 10.1111/j.1462-2920.2007.01324.x